International Journal of Applied Earth Observation and Geoinformation 140 (2025) 104599

Contents lists available at ScienceDirect

International Journal of Applied Earth Observation and Geoinformation

journal homepage: www.elsevier.com/locate/jag

How can we improve data integration to enhance urban air temperature estimations?

Zitong Wen [a,*], Lu Zhuo [a,b,*], Meiling Gao [c], Dawei Han [a]

[a] Department of Civil Engineering, University of Bristol, Bristol BS8 1TR, UK
[b] School of Earth and Environmental Sciences, Cardiff University, Cardiff CF10 3AT, UK
[c] College of Geological Engineering and Geomatics, Chang'an University, Xi'an 710054, China

ARTICLE INFO

Keywords:
Air temperature
High resolution
Data integration
Weather radar
Crowdsourced weather station

ABSTRACT

High-resolution urban air temperatures are indispensable for analysing excess mortality during heatwaves. As a crucial method for obtaining high-resolution data, multi-source data integration has been widely used in urban temperature estimations. However, current research predominantly focuses solely on integrating official weather station observations, satellite products, and reanalysis datasets. Despite the significant cooling effect of rainfall on air temperatures, no studies have explored the contribution of rainfall-related variables to high-resolution air temperature estimations. Additionally, due to the scarcity of official weather stations, quantifying the impact of station density remains an underexplored research direction. To tackle these challenges, we innovatively integrated satellite products, reanalysis datasets, and weather radar data with air temperature observations from crowdsourced weather stations. Using genetic programming, we developed statistical downscaling models to estimate high spatiotemporal resolution (1-km, hourly) air temperatures in London during the summers of 2019 and 2022. The models achieved *RMSEs* of 1.694 °C (2019) and 1.785 °C (2022), *R-squared* values of 0.867 and 0.862, and *MAEs* of 1.276 °C and 1.278 °C, respectively. Notably, the accuracy of the models was found to improve with increased weather station density, particularly when the density was below 0.5 stations per 100 km^2. Moreover, high-resolution rainfall observations significantly impacted the accuracy of air temperature estimations, second only to elevation, highlighting the potential of integrating radar data. These findings can provide valuable insights for scholars aiming to improve data integration for enhancing urban air temperature estimations.

1. Introduction

Climate change has led to an increasing frequency of extreme weather events around the world (Clarke et al., 2022). Heatwaves, as one of the deadliest extreme weather events(Vautard et al., 2020), have received considerable attention from the academic community and the general public due to their significant impact on resident health and urban sustainable development (Macintyre et al., 2018). Many heat-related mortalities have been recorded in the UK (Arbuthnott & Hajat, 2017), the USA (Anderson & Bell, 2011), China (Yin & Wang, 2017), and France (Fouillet et al., 2008). An analysis conducted in 2017 indicated that approximately 30 % of the residents worldwide are exposed to lethal high temperatures for at least 20 days annually (Mora et al., 2017). This percentage is likely to exceed 48 % by 2100. To assess the impact of heatwaves and analyse the feasibility of countermeasures, it is indispensable to monitor distributions of heatwaves at a high spatiotemporal resolution, providing theoretical support for heatwave-related studies.

Air temperature, as one of the most commonly used indicators, is widely used in defining and monitoring heatwaves (Z. Xu et al., 2016). Heat-related mortality studies require high-resolution air temperature data to link death records to local area factors such as land-use type and topography (Murage et al., 2020). However, since weather stations can only capture air temperatures at point locations and are only scarcely available at the city level, obtaining high spatiotemporal resolution air temperatures has become a challenge. To tackle this issue, many studies have explored using satellite products of land surface temperature (LST) to retrieve high-resolution gridded air temperatures. Vancutsem et al. (2010) utilised MODIS LST products to retrieve daily 1-km air temperatures in Africa, achieving relatively good performance with a root mean

* Corresponding authors at: Department of Civil Engineering, University of Bristol, Bristol BS8 1TR, UK.
E-mail addresses: bq22490@bristol.ac.uk (Z. Wen), zhuol@cardiff.ac.uk (L. Zhuo).

https://doi.org/10.1016/j.jag.2025.104599
Received 4 June 2024; Received in revised form 8 May 2025; Accepted 10 May 2025
Available online 17 May 2025
1569-8432/

square error (*RMSE*) of 2.4 °C. The study by Yoo et al. (2018) further demonstrated the feasibility of estimating high-resolution urban daily maximum temperatures based on satellite LST products. However, most satellites can only observe surface conditions during overpassing times, and cloud cover adds another layer of hindrance to data availability (Shen et al., 2016). Thus, it is hard to provide temporally continuous air temperature observations at the city level based on satellite products. Also, air temperature retrievals based on satellite products often require sufficient weather station observations for downscaling model training and validation. Otherwise, the lack of weather stations in urban areas hinders the effective capture of spatial variability caused by factors such as land cover, building characteristics, and vegetation density (Saaroni & Ziv, 2010). Some scholars have attempted to overcome this limitation by adopting high-density temperature monitoring networks (Bassett et al., 2016) or mobile sampling of air temperatures (Tsin et al., 2016). However, the current installation and maintenance costs of these methods are prohibitively high. In recent years, there has been increasing attention to the utilisation of crowdsourced air temperature data to compensate for the limited observations from official weather stations. Crowdsourced air temperature data, observed and uploaded by private weather stations, is considered to have significant potential for monitoring urban thermal environments (Meier et al., 2017). Due to its efficiency and cost-effectiveness, air temperature observations from crowdsourced weather stations have become an important data source for sampling efforts of temperature-related research (Mitchell & Fry, 2024).

The integration of multi-source data to construct statistical regression models is an effective approach for generating high spatiotemporal resolution air temperatures. The fusion of satellite remote sensing and crowdsourced air temperature data has been proven to have great potential for monitoring spatial distributions of air temperatures in urban areas (Venter et al., 2020). However, current literature mainly focused on the fusion of satellite remote sensing, reanalysis models, and crowdsourced weather station observations (Brousse et al., 2022; Gutiérrez-Avila et al., 2021; Hassani et al., 2023). The exploration of integrating weather radar rainfall observations on high-resolution air temperature estimations is very limited. Weather radar observations can provide real-time coverage of rainfall data with high spatiotemporal resolution (Sokol et al., 2021). The cooling effect of rainfall on air temperature has already been confirmed in many studies (W. Liu et al., 2022; Rooney et al., 2018). Kodama et al. (2024) have also demonstrated the important role of station-based rainfall data in improving the accuracy of air temperature estimation. Despite its potential, to our knowledge, no study has explored integrating rainfall data from weather radar into air temperature estimations.

Determining how variations in weather station density affect the performance of statistical air temperature models has always been one of the primary challenges faced in climatological statistical research. In most cases, due to the sparse distribution of weather stations, the limited density of weather stations can result in increased errors when generating gridded air temperatures (J. Wang et al., 2014). This is because sparse stations may fail to adequately represent all land use types within the study area (M. Wang et al., 2024). However, although the weather station density has been shown to correlate with the accuracy of climate models (Njoku et al., 2023), the quantification of the impact of weather station density has not been the focus of previous studies. For instance, when Dos Santos (2020) estimated the maximum daily temperatures in London, the study only expanded the study area to include more meteorological stations as a response after subjectively assessing the lack of station observations. A similar sampling strategy can also be observed in the study by Oswald et al. (2024), where the spatial extent was adjusted primarily to ensure the inclusion of sufficient station data. Neither research delved into the specific effects of station density on model performance. Therefore, testing what weather station density can meet the requirements for estimating high spatiotemporal resolution air temperatures could be beneficial. Furthermore, while comparing the performance of different methods, previous studies have often simply compared the numerical performance of the proposed models with that of previous studies (Flückiger et al., 2022; Kloog et al., 2014; Yan et al., 2009). It also overlooked the impact of varying weather station densities on the model.

To address the research gap, we explored the potential of integrating data from satellite products, reanalysis dataset, weather radar, and crowdsourced weather stations to generate high spatiotemporal resolution air temperatures in this study. The research utilised a genetic programming (GP) algorithm to integrate multi-source data for training and validating the statistical downscaling regression model to generate hourly 1-km air temperatures. London was selected as the study area considering its frequent occurrence of extreme heatwaves. Given that heat-related mortality often occurs during the daytime and daily maximum temperature serves as the criterion for UK heatwave identification, the daytime periods of summer 2019 and 2022 were selected as the study period for estimating hourly air temperatures. The study aimed to evaluate how the obtaining of high spatiotemporal resolution air temperatures is influenced by (1) local-scale variables, (2) rainfall, and (3) weather station density. The resulting high-resolution temperature maps can provide urban planners and public health authorities with more accurate and fine-grained information to identify heat-vulnerable areas and design targeted mitigation strategies.

2. Study area

Residents are particularly vulnerable to the adverse effects of high temperatures, posing a threat to health when temperatures exceed 19 °C in urban areas (Hajat et al., 2002). London, as the largest city in the UK, boasts a population of over 9 million residents, with an average density of 5700 residents per square kilometre. Over the past few decades, London has experienced numerous heatwave events, with the frequency steadily increasing (Sanderson et al., 2017). Notable heatwaves affecting London occurred in 2013, 2019, 2020, and most recently in 2022 (Green et al., 2016; Rustemeyer & Howells, 2021; Thompson et al., 2022; Yule et al., 2023). Therefore, this study focuses on London, the area between latitudes 51.7° and 51.2°N and longitudes 0.5°W and 0.4°E, as shown in Fig. 1. This area is described using the local climate zone classification, which is a systematic classification scheme for effectively describing various types of urban landscapes and built-up areas. The summer of 2019 and 2022 (June to August) was chosen as the study period for this research, considering the relatively high occurrence of heatwaves in London during these years, with three events recorded in 2019 and multiple extreme temperature episodes in 2022.

3. Data products

Four sources of data were integrated into this study, including earth observation satellite data, weather radar observations, reanalysis dataset, and crowdsourced weather station observations. The data products used in this research are summarised in Table 1.

3.1. Earth observation satellite data

All earth observation satellite data were obtained and pre-processed on the Google Earth Engine (GEE) cloud-computing platform (Gorelick et al., 2017). The satellite products utilised include the Terra MODIS, the NASA SRTM, and Landsat 8 OLI. All available scenes observing London were collected and utilised, with the 'pixel_qa' band and 'detailedQA' band employed to eliminate data obscured by cloud cover. The detailed information on satellite products obtained from these datasets is shown in Table 1.

By providing shade and through evapotranspiration, vegetation can effectively reduce air temperatures in urban areas (Shiflett et al., 2017). Therefore, green infrastructure has been widely implemented in major cities to cope with extreme heat events (Koc et al., 2018). NDVI, an index

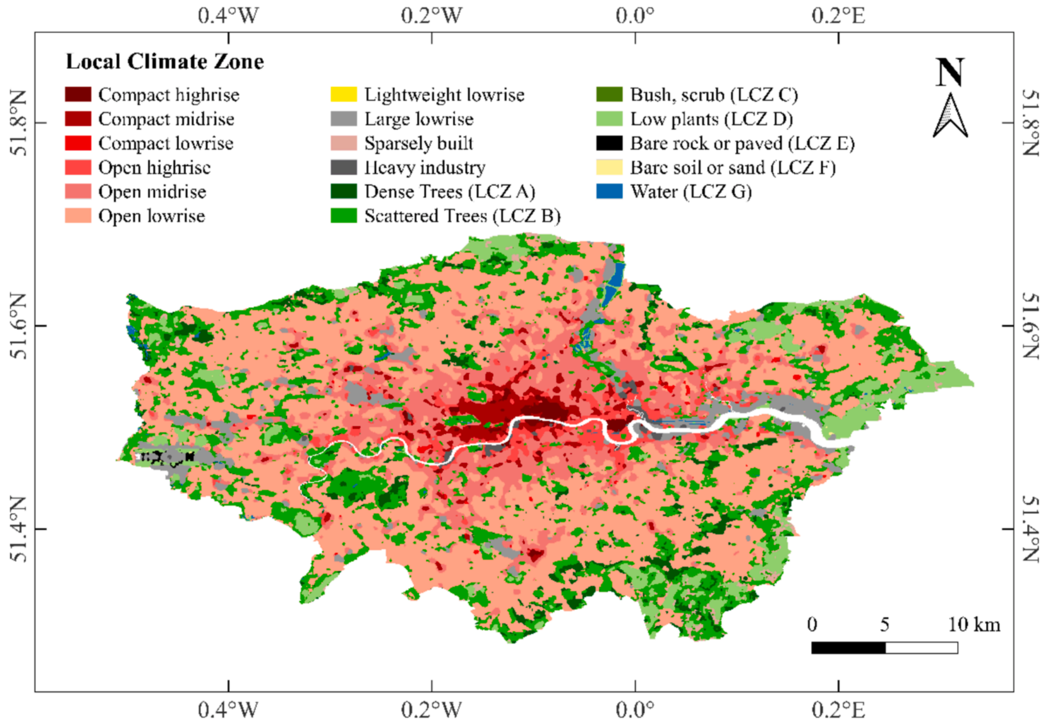

Fig. 1. Map of the study area with local climate zone.

Table 1
Summary of data products utilised in constructing the statistical downscaling model for air temperatures in London.

Variable	Data source	Temporal Resolution	Spatial Resolution
Normalised difference vegetation index (NDVI)	Moderate resolution imaging spectroradiometer (MODIS)	16 days	1 km
Emissivity (band 31)		8 days	
Modified normalised difference water index (MNDWI)	Landsat 8 operational land imager (Landsat 8 OLI)	16 days	30 *m*
Elevation	Shuttle radar topography mission (SRTM)	/	90 *m*
Rainfall	UK Met Office NIMROD system	Hourly	1 km
Soil moisture (0–7 cm)	Land component of the ECMWF ERA5 climate	Hourly	$0.1^{\circ} \times 0.1^{\circ}$
2-m air temperature	reanalysis (ERA5-Land)	Hourly	
Station-based air temperature	Weather observations website (WOW)	Hourly	Point

used to detect vegetation presence and estimate vegetation cover, has been widely recognized in previous studies for its importance in air temperature estimation (Shen et al., 2020; Zhou et al., 2020). In fact, it consistently ranks among the top 50 % of selected explanatory variables in terms of influence on estimation accuracy. Although the temperature-vegetation index (TVX) method allows NDVI to be used independently for estimating air temperature, its failure to account for other topographical parameters can lead to significant errors (Zhu et al., 2013). Therefore, in this study, NDVI from MODIS product was adopted to quantify the impact of vegetation on air temperatures while considering additional influencing factors. Morning atmospheric interference is generally lower than in the afternoon which can result in more reliable data quality and consistency. Considering that MODIS Aqua's daytime view time over London is 2:00 PM, this study adopts the MODIS Terra NDVI product whose daytime view time was 11:00 AM was adopted in this research. It can be freely accessed at https://developers.google.com/earth-engine/datasets/catalog/MODIS_061_MOD13A2.

Emissivity is the ratio of the energy radiated from the surface of a material to that radiated from a blackbody. The value of emissivity largely depends on the properties, geometry, composition, and roughness of the land (Stathopoulou et al., 2007). For instance, due to the trapping effect of street canyons on longwave radiation (Ferreira et al., 2012), the surface emissivity in urban areas is slightly lower than that of natural landscapes. It is one of the reasons leading to relatively higher air temperatures in urban areas. Thus, many studies utilised emissivity to explore the impact of different land covers on air temperatures (Wen et al., 2023). Compared to other bands of MODIS, the influence of atmospheric water vapour and temperature profile variations within the spectral range of MODIS band 31 (10.78–11.28 μm) is smallest, as well as the uncertainty (Coll et al., 2009). Thus, Terra MODIS band 31 was adopted in the study to quantify the energy absorption capacity of different land covers, accessible at https://developers.google.com/earth-engine/datasets/catalog/MODIS_061_MOD11A2. However, given that water bodies and green vegetation share similar emissivity, an additional explanatory variable is needed to analyse the impact of water bodies on air temperature estimations.

Due to its high thermal inertia, high evaporation rate, and lower surface temperature, water bodies can contribute to cooling their surrounding areas (Hong et al., 2023), especially during the hottest periods of the day. Wen et al. (2023) found that water bodies ranked as the third most important factor in air temperature estimation, further supporting their significant contribution. Similarly, in the study by (Carrión et al., 2021), the influence of water bodies on air temperature estimation was also ranked among the top 50 % of all explanatory variables. Previously, NDWI has been used as an explanatory variable to represent water bodies. However, MNDWI is more effective in suppressing or even eliminating noise from built-up areas, vegetation, and soil (H. Xu, 2006), making it better suited for detecting water bodies in urban environments. Therefore, MNDWI was adopted in this study to monitor water body variations, which can be accessed at https://developers.google.

com/earth-engine/datasets/catalog/LANDSAT_LC08_C02_T1_L2.

Elevation is recognised as one of the important factors influencing air temperature, and the typical temperature lapse rate is often considered 6.5 °C/km. Although elevation data is generally regarded as fixed and unchanging, making it unsuitable for directly estimating air temperature, numerous previous studies have identified it as the most critical factor in air temperature estimations (Didari & Zand-Parsa, 2018; Shi et al., 2016). Therefore, in this study, we utilize the SRTM Digital Elevation Model (DEM) to obtain detailed elevation data for the study area and assess its impact on air temperature estimations. This dataset is available at https://developers.google.com/earth-engine/datasets/catalog/CGIAR_SRTM90_V4/.

3.2. Weather radar observations

Due to the evaporation of water, raindrops can effectively cool the surrounding air when they fall into unsaturated air. While many studies have reported a negative correlation between air temperature and rainfall (Abera et al., 2020; W. Liu et al., 2022), no study has incorporated rainfall data into air temperature estimations. To accurately assess the impact of rainfall on air temperature estimations, this study utilizes 1-km hourly rainfall observations derived from weather radar data processed by the UK Met Office's NIMROD system for the London region. Detailed information on the rainfall data can be found in Table 1. It can be freely accessed at https://catalogue.ceda.ac.uk/uuid/27dd6ffba67f667a18c62de5c3456350. However, this dataset can only monitor real-time rainfall data and cannot capture the prolonged cooling effect of residual rainwater in the soil on air temperature (Roshan & Moghbel, 2020).

3.3. Reanalysis data

All reanalysis data in this study were obtained from ERA5-Land. As a reanalysis dataset, ERA5-Land is released by the European Centre for Medium-Range Weather Forecasts (ECMWF). Compared to ERA5, it provides a higher resolution and offers a consistent view of the development of land and atmospheric variables from 1950 to the present, which can be freely accessible at https://cds.climate.copernicus.eu/cdsapp#!/dataset/reanalysis-era5-land?tab = overview. Detailed information on the reanalysis data used in the study can be found in Table 1.

Soil moisture is considered an effective indicator for capturing the cooling effect of residual water in the soil on air temperature. This was further confirmed in the study by X. Zhang et al. (2022), where soil moisture was identified as the fourth most important explanatory variable in air temperature estimation. Despite its recognized importance, soil moisture has rarely been incorporated into air temperature estimation models. To assess its significance, this study utilizes soil moisture data obtained from ERA5-Land. Given that heat exchange with the atmosphere primarily occurs at the soil surface, only soil moisture data from the 0–7 cm layer was considered in this study.

Many studies have demonstrated the reliability and accuracy of ERA5-Land in estimating air temperature (Almeida & Coelho, 2023; Yilmaz, 2023; Zhao et al., 2023). Although its spatial resolution ($0.1^\circ \times 0.1^\circ$) may not be sufficient for local-scale studies, its high temporal resolution (hourly) makes it widely recognized as a suitable larger-scale variable for air temperature statistical downscaling models (Wen et al., 2023; Y. Zhang et al., 2024). Therefore, the 2-m air temperature data from ERA5-Land was used as the coarse-resolution input for air temperature statistical downscaling models in this study.

3.4. Weather station observations

Weather observations website (WOW), a global network of crowdsourced weather observations, provides open access to weather data from both the citizen science community and Met Office weather stations. Scholars can freely access meteorological observations by joining the WOW network, which is available at https://wow.met.ie/. In this research, air temperature observations from WOW weather stations within London were used as reference data for statistical downscaling models of air temperatures. In 2019, data from 63 WOW stations were utilized, while in 2022, 66 stations were available. The main weather station models used were Davis Vantage Pro2 and Fine Offset WH1080, which have reported uncertainty ranges of ± 0.3 and ± 0.5 ℃, respectively. The details of air temperatures from WOW can be seen in Table 1, and Fig. 2 illustrates the distribution of crowdsourced weather stations in London. This study retrieved hourly air temperature data from all available stations for all available dates between June 1 and August 31 in 2019 and 2022, along with their latitude and longitude coordinates.

However, due to non-traditional measurement equipment and inconsistent installation setups, the quality of observations from private weather stations remains problematic (Chapman et al., 2017; Napoly et al., 2018). Therefore, the use of data from private weather stations requires quality control (QC) to eliminate gross errors and correct instrument biases at specific stations. In this study, the following QC process was utilised to identify and remove potential outliers:

1) Range test

To detect whether air temperature observations fall outside a reasonable range, a range check is necessary during the QC process. Considering that the upper and lower extremes of air temperature vary across different climatic regions, this study utilised the range check established by the UK Met Office to detect outliers. All air temperature observations outside the range of −26 ℃ and 37 ℃ were identified. However, not everything outside these limits was incorrect. If observations from nearby Met Office weather stations also verified this phenomenon during the same period, the value was considered valid; otherwise, the record was removed. As a result, 0.13 % of the observations were removed in 2019, while 0.09 % were removed in 2022.

2) Step test

After a brief interruption in connection to the receiver, temperature data recorded by weather stations may exhibit sharp increases or decreases (WMO, 1993). Therefore, to identify unrealistic jumps in the observed data, the step test was employed to ensure that the magnitude of change between consecutive observations falls within a certain range. According to the standards of the UK Met Office, this study removed values where the difference between the value and its previous value exceeds ± 5 °C. Consequently, 0.52 % of the dataset was removed in 2019, while 0.57 % was removed in 2022.

3) Stuck test

To detect weather stations with connectivity issues, a persistence test is commonly employed. This test identifies stations that repeatedly transmit the same observed values (Cerlini et al., 2020). In this study, observed values that remained unchanged within a 6-hour period were removed according to the stuck test from the UK Met Office. As a result, 0.04 % of the dataset was removed in 2019, while 0.11 % was removed in 2022.

4) Spatial outliers

Due to non-traditional installation setups, observations from some private weather stations may exhibit significant discrepancies compared to the actual conditions within the study area. Therefore, detecting spatial outliers in the observational data is necessary. This study addressed this issue by removing any weather stations found to deviate from the daily mean of all stations by more than one standard deviation. In both 2019 and 2022, data from one weather station were removed, accounting for 2.25 % of observations in 2019 and 1.89 % in 2022.

Finally, after applying the above QC measures, a total of 53,776 hourly air temperature observations from 62 weather stations were used for 2019, while 62,915 observations from 65 stations were utilized for 2022.

3.5. Data pre-processing

Due to the varying spatial and temporal resolutions of the data

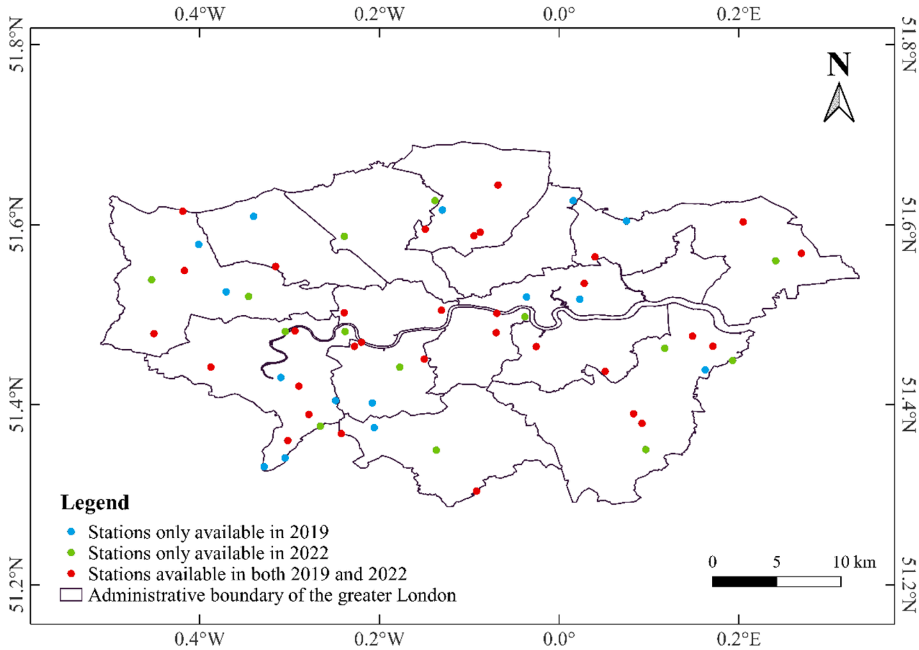

Fig. 2. The distribution map of crowdsourced weather stations in London.

products used in this study, preprocessing steps are necessary. For all data products, the spatial resolution was standardized to match the 1-km resolution of MODIS Terra products within GEE. Specifically, the conversion set the 1-km resolution of the MODIS product as the target and spatially aligned to the same pixel boundaries. High-resolution products with resolutions better than 1 km are aggregated to 1 km, while coarser-resolution products with resolutions larger than 1 km are reprojected to 1 km. Air temperatures from weather stations were considered to represent the air temperature of the 1-km pixel where it was located.

For temporal resolution preprocessing, considering that satellite observations of variables like NDVI, emissivity, MNDWI, and elevation change slowly compared to air temperature, many studies often assumed that these variables observed by satellites were static over a period (Dos Santos, 2020; Kaplan et al., 2019). Therefore, this study utilised monthly averaged values of these variables extracted through GEE to represent the conditions of the month.

4. Methodology

4.1. Regression models

In this study, stepwise linear regression was initially employed to rank the significance and investigate the potential contribution of each local-scale variable to the downscaling of air temperature. Based on the ranking of variables obtained from stepwise linear regression, the study created 6 groups to assess the impact of fusing different local-scale

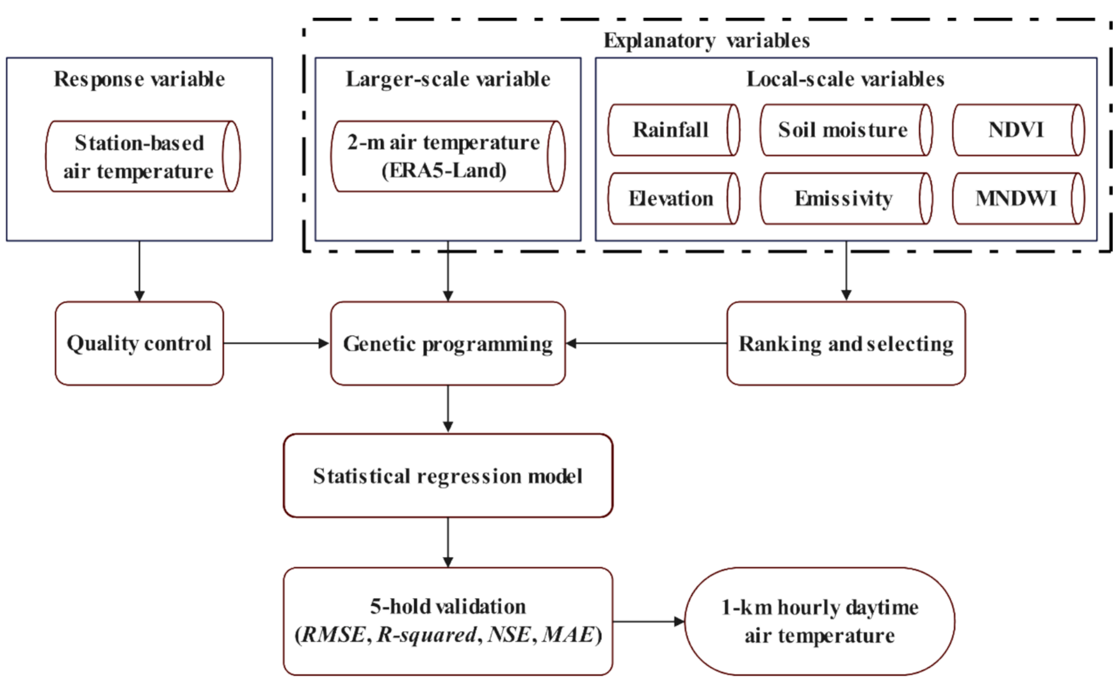

Fig. 3. The flowchart of the statistical downscaling model for air temperature.

variables on air temperature downscaling. These 6 groups were constructed starting from the variable with the maximum standardised coefficient (*Beta*). Beta is derived by multiplying the unstandardised coefficient (*B*) by the ratio of the standard deviation of the independent and dependent variables. A higher absolute value of Beta indicates that the independent variable has a more substantial impact on the dependent variable. Subsequently, adding one variable at a time according to the ranking until all variables were included. All groups were evaluated based on the performance of the generated downscaling model to assess the impact of integrating different local-scale variables on the accuracy of air temperature downscaling. Considering that the 2-m air temperature from ERA5-Land was utilised as the coarse-resolution variable for the downscaling model in this study, it was included in all of the testing groups. The overall framework of the model can be seen in Fig. 3.

Our study chose to utilise the GP algorithm (Abonyi, 2022), a supervised machine learning technique, to obtain an appropriate downscaled regression model for estimating air temperature with high spatiotemporal resolution. The GP algorithm, depicted in Fig. 4, can effectively integrate observed multi-source data by constructing symbolic regression models in the form of binary trees to generate interpretable statistical regression models, which has been proven to outperform ordinary least squares (OLS) regression and artificial neural networks (ANN) (Gandomi & Roke, 2015; Gomes et al., 2019). In this study, NDVI, MNDWI, elevation, emissivity, rainfall, surface soil moisture (0–7 cm), and 2-meter air temperature from ERA5-Land are utilised as explanatory variables in the proposed model, as shown in Fig. 3. Among these, 2-meter air temperature from ERA5-Land serves as the larger-scale variable in the statistical downscaling model, while the other variables serve as local-scale variables. The hourly air temperature observed by crowdsourced weather stations was used as the response variable of the model.

4.2. Effect of weather station density

This study employed an iterative approach to assess the influence of weather station density on the accuracy of the downscaling model. For 2019, weather stations were randomly removed from the training dataset in increments of 5 stations, reducing the total from 62 to 7. Similarly, for 2022, the number of stations was iteratively reduced from 65 to 5. For each increment, the optimal variable group obtained from Section 4.1 was utilised in executing the GP algorithm to generate the downscaling regression model. Then, the research used 5-fold CV to evaluate the performance of the model generated in each iteration and linked these with the density of weather stations.

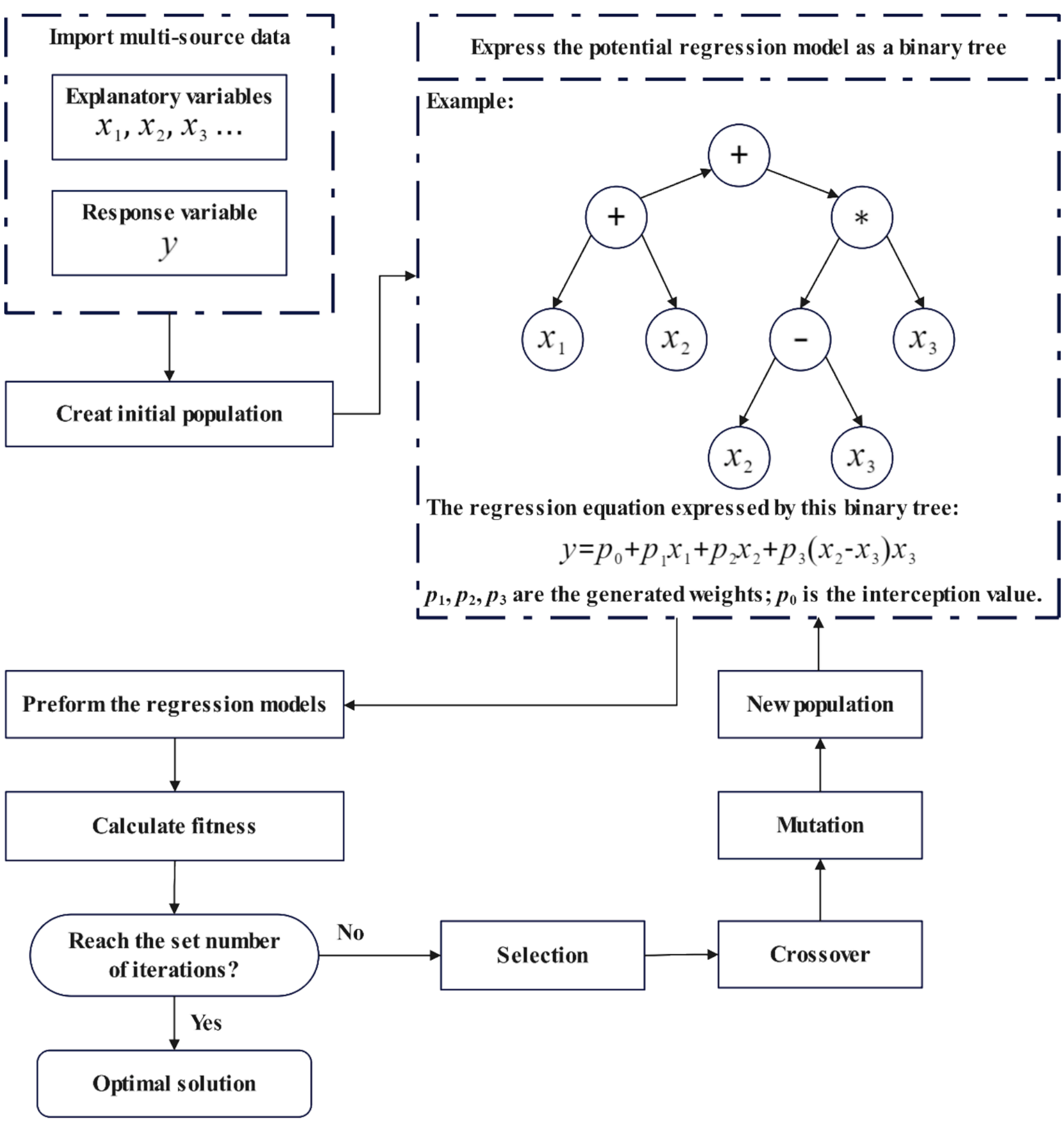

Fig. 4. The workflow of the GP algorithm.

4.3. Model validation and accuracy

To validate the accuracy of the regression model, our study adopted 5-fold CV to assess the performance of the generated air temperature data. In 5-fold CV, the data samples are randomly divided into five equally sized sample subsets. Four of these subsets were used to train the downscaling regression model, while the remaining subset was used to evaluate the trained model (Z. Zhang & Du, 2022). The process was repeated until each subset had been used for validation, resulting in five rounds of training and validation.

Three commonly used statistical indicators in synoptic meteorology were adopted in this study to evaluate the performance of the model, including the coefficient of determination (*R-squared*), mean absolute error (*MAE*), and *RMSE*. The equations are as follows:

$$R - squared = \left(\frac{cov(o,s)}{\sigma_o\sigma_s}\right)^2 \tag{1}$$

$$MAE = \frac{\sum_{t=1}^{T}\left|y_o^t - y_s^t\right|}{T} \tag{2}$$

$$RMSE = \sqrt{\frac{\sum_{t=1}^{T}\left(y_o^t - y_s^t\right)^2}{T}} \tag{3}$$

in which y_o^t and y_s^t represent observed air temperature and air temperature from the regression model at time t, respectively. σ_o and σ_s are the standard deviation of observations and the regression model, respectively. $cov(o,s)$ is the covariance between air temperature observations and air temperature from the regression model.

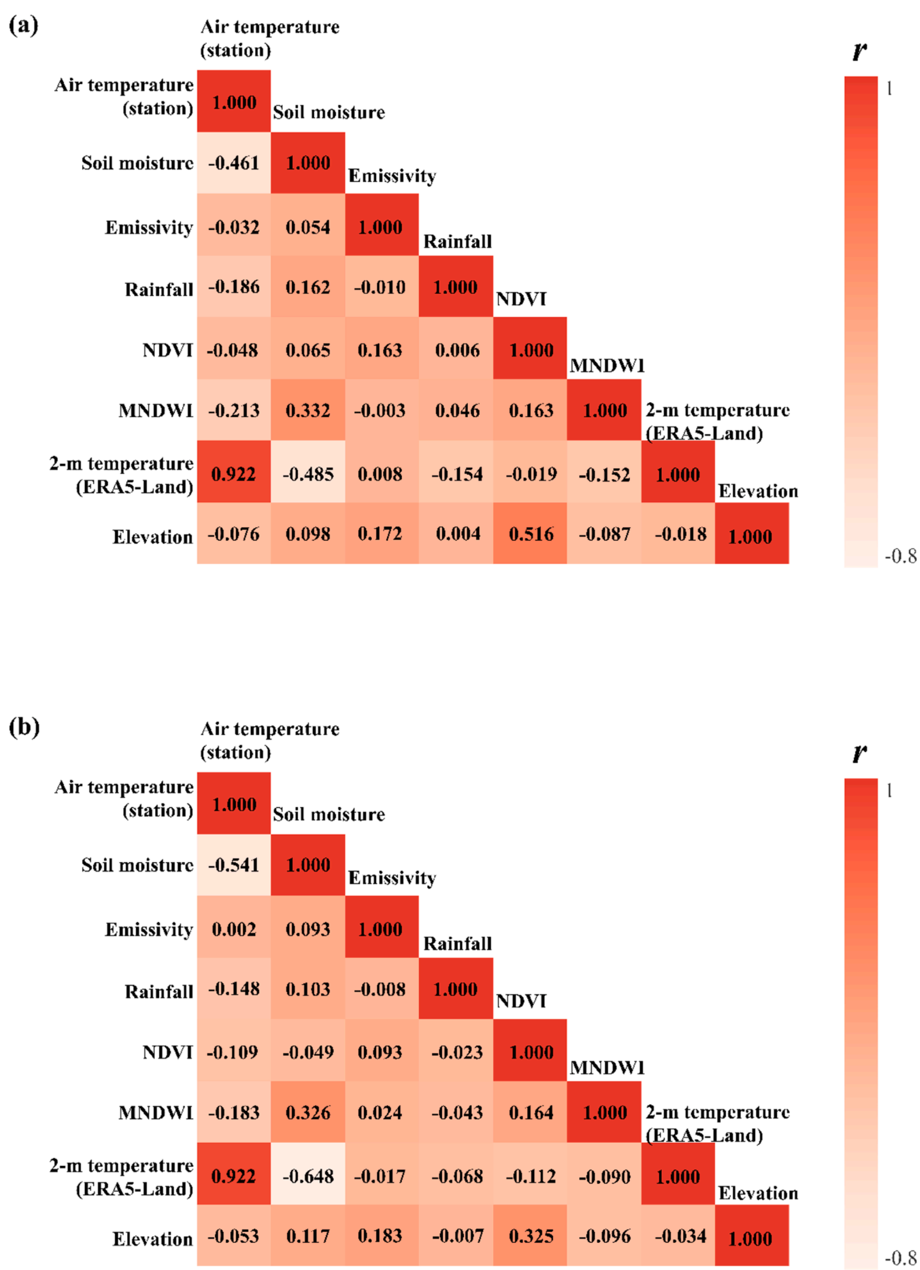

Fig. 5. Pearson correlation (r) between the explanatory variables and air temperature observations from weather stations: (a) 2019; (b) 2022.

5. Results

5.1. Local-scale variables contribution

Pearson correlation (*r*) was calculated in this research to assess the correlation between all explanatory variables and the hourly air temperature observations from the weather stations, as shown in Fig. 5. Soil moisture shows the highest degree of correlation among all local-scale variables with hourly air temperature observations, with a negative correlation coefficient of 0.461 in 2019 and 0.541 in 2022. Following closely is MNDWI, displaying a negative correlation coefficient of 0.213. As the third most correlated local-scale variable, rainfall demonstrates a negative correlation of 0.186 in 2019 and 0.148 in 2022, showing greater relevance compared to NDVI, elevation, and emissivity, which have been frequently used as explanatory variables in regression models in previous studies (Dos Santos, 2020; Lin et al., 2012; Noi et al., 2016).

Subsequently, the forward stepwise regression approach was employed to create a ranking, starting from the explanatory variable with the maximum *Beta*-value, up to all variables under consideration. Table 2 presents the results of the stepwise regression. Both the 2019 and 2022 results indicate that elevation was identified as the most important explanatory variable among local-scale variables for achieving higher spatiotemporal resolution, followed by rainfall. Considering both years together, MNDWI can be considered as the third most influential factor. The *t*-value and *p*-value, signifying the significance of the variables, are also utilised and demonstrate results consistent with the ranking based on the *Beta*-value in the study. It is also worth noting that, despite slight differences in rankings compared to Fig. 5, the influence of rainfall in the downscaling model is still considered higher than that of variables such as NDVI used in previous studies. Moreover, although soil moisture shows a high correlation in Fig. 5, the results in Table 2 show that it does not contribute to the regression model performance as expected.

Based on the ranking of local-scale variables in Table 2, 6 groups of variables were created to generate regression models using the GP algorithm: starting from the most correlated local-scale variable, which in this research was elevation, one variable was added at a time according to the ranking until all local-scale variables were included. To evaluate the performance of the regression models generated by these six groups, a total of 53,776 samples of hourly air temperature observations from weather stations were used for 2019, while 62,915 samples were utilized for 2022.

Table 2
Stepwise regression results for the model with all explanatory variables.

2019 summer	Unstandardised Coefficients		*Beta*	*t*	*ρ*
	B	Std. Error			
(Constant)	31.146	1.756	/	17.739	0.000
2-m temperature (ERA5-Land)	1.132	0.002	0.916	486.307	0.000
Elevation	−0.008	0.000	−0.055	−28.821	<0.001
Rainfall	−0.426	0.016	−0.044	−26.753	<0.001
Emissivity	–32.842	1.809	−0.030	−18.154	<0.001
MNDWI	0.672	0.060	0.020	11.178	<0.001
Soil moisture	−0.668	0.158	−0.008	−4.241	<0.001
NDVI	0.231	0.071	0.006	3.239	0.001
2022 summer	**Unstandardised Coefficients**		***Beta***	***t***	***ρ***
	B	**Std. Error**			
(Constant)	15.718	3.045	/	5.161	<0.001
2-m temperature (ERA5-Land)	1.129	0.003	0.911	352.101	0.000
Elevation	−0.007	0.000	−0.050	−19.377	<0.001
Rainfall	−0.461	0.022	−0.047	−20.692	<0.001
MNDWI	0.803	0.117	0.020	−6.854	<0.001
NDVI	−0.760	0.082	−0.023	9.254	<0.001
Emissivity	−16.209	3.162	−0.013	−5.126	<0.001
Soil moisture	−0.918	0.217	−0.011	−4.237	<0.001

For better comparison, Table 3 presents the performance metrics of the downscaling regression models generated by the 6 groups. As local-scale variables are added, the performance of the generated air temperature downscaling models also steadily improves. Group 6, which included all local-scale variables, produced the best-performing downscaling regression model. For 2019, it achieved an *R-squared* value of 0.867, an *RMSE* of 1.694 °C, and an *MAE* of 1.276 °C, while for 2022, the model attained an *R-squared* value of 0.862, an *RMSE* of 1.785 °C, and an *MAE* of 1.278 °C. This study selected three representative weather stations to illustrate temporal variations of the optimal model, as shown in Fig. 6. The high consistency between the downscaling model and weather station observations demonstrates that our generated downscaling model can accurately estimate air temperatures with high spatiotemporal resolution. Fig. 7a illustrates the spatial distribution of air temperature in London at 14:00 on July 4, 2019, derived from the downscaling model generated by Group 6. The white pixels observed in the River Thames result from the missing data in the emissivity satellite products at the river estuary, which can be seen in Fig. 7d. Associated with the local climate zone in Fig. 1, it can be noted that most areas with air temperatures above 25 °C are located in the city centre (e.g., the City of London and Westminster) or residential areas (e.g., Wood Green, Woolwich, Walthamstow, Morden, Peckham, Hounslow, and Earling). By combining Fig. 7a with Fig. 7d-f, it becomes evident that areas in urban regions characterised by low emissivity, such as water bodies and highly vegetated parks, generally exhibit lower air temperatures. Other low air temperature areas are primarily found in higher elevation areas such as Addington Hills, as shown in Fig. 7c. However, the study also observed that Jubilee Wood Local Nature Reserve and Southall, located away from urban and residential areas, present unusually high air temperatures. Similar phenomena are also found in the spatial distribution of 2-m temperature from the ERA5-Land dataset, as shown in Fig. 7b.

Moreover, it is worth noting that the performance of these 6 groups exhibits a similar phenomenon to the significance ranking obtained from stepwise linear regression results (Table 2): the higher the ranking of local-scale variables, the greater their impact on the performance of the

Table 3
Performance of 6 groups of explanatory variables for air temperature downscaling.

Year		Adopted local-scale variables	*R-squared*	*RMSE*	*MAE*
2019	Group (1)	Elevation	0.842	1.897	1.442
	Group (2)	Elevation + Rainfall	0.862	1.726	1.297
	Group (3)	Elevation + Rainfall + Emissivity	0.866	1.701	1.282
	Group 4	Elevation + Rainfall + Emissivity + MNDWI	0.866	1.696	1.279
	Group 5	Elevation + Rainfall + Emissivity + MNDWI + Soil moisture	0.866	1.693	1.277
	Group 6	Elevation + Rainfall + Emissivity + MNDWI + Soil moisture + NDVI	0.867	1.694	1.276
2022	Group (1)	Elevation	0.839	1.948	1.373
	Group (2)	Elevation + Rainfall	0.848	1.897	1.342
	Group (3)	Elevation + Rainfall + MNDWI	0.856	1.851	1.319
	Group 4	Elevation + Rainfall + MNDWI + NDVI	0.860	1.815	1.297
	Group 5	Elevation + Rainfall + MNDWI + NDVI + Emissivity	0.861	1.796	1.292
	Group 6	Elevation + Rainfall + MNDWI + NDVI + Emissivity + Soil moisture	0.862	1.785	1.278

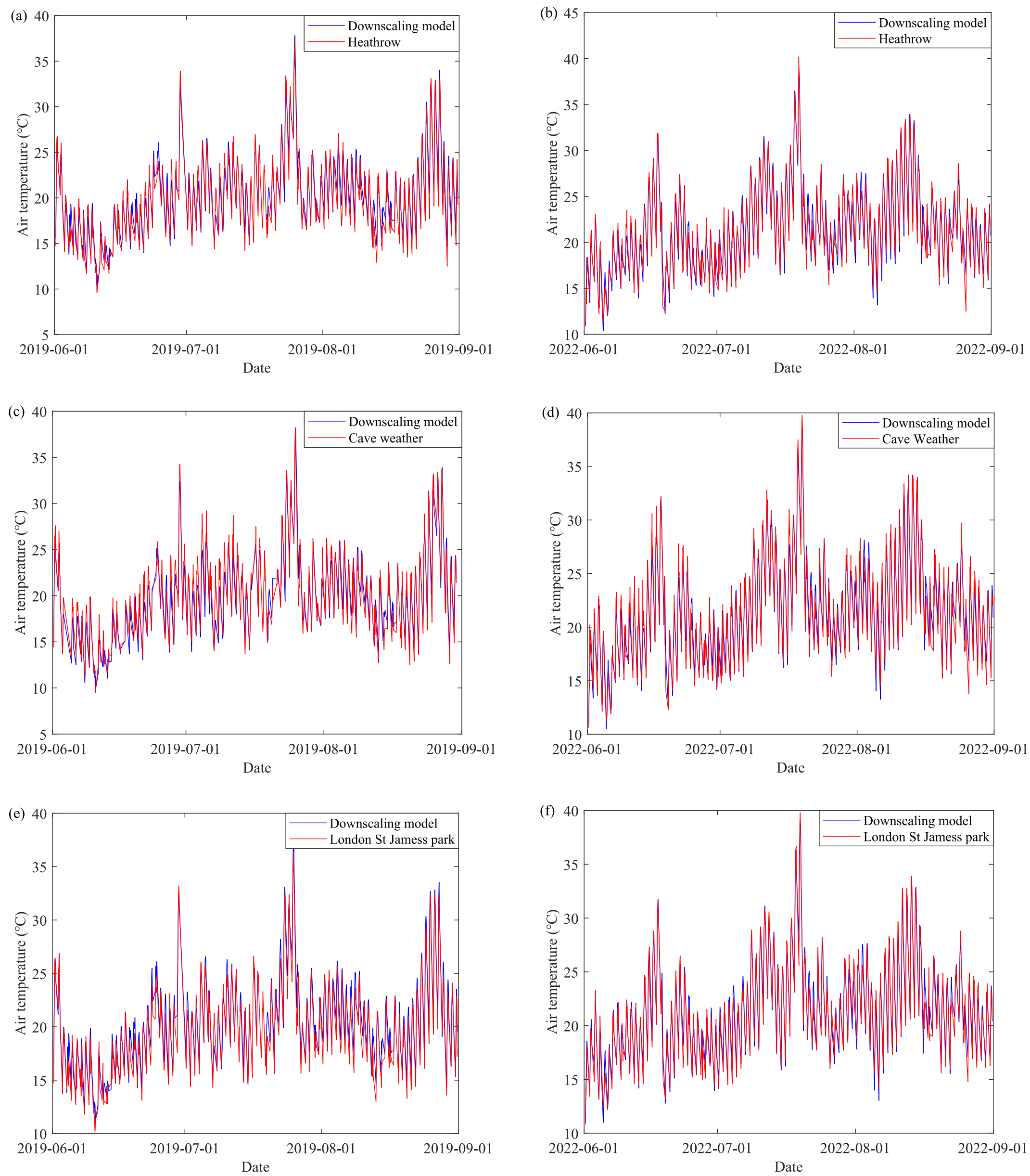

Fig. 6. Temporal variations of hourly air temperature during daytime (6:00–18:00): (a) Heathrow (2019); (b) Heathrow (2022); (c) Cave Weather (2019); (d) Cave Weather (2022); (e) London St James's Park (2019); (f) London St James's Park (2022).

downscaling regression model. For example, in 2019 summer, the addition of the second-most relevant variable, rainfall, resulted in a decrease of 0.171 °C in the *RMSE* of the regression model compared to Group (1). Meanwhile, the addition of the fifth-most relevant variable, soil moisture, only led to a reduction of 0.003 °C in the *RMSE* compared to Group 4. Moreover, the study unexpectedly found that the MNDWI, representing water bodies, contributed more significantly to air temperature estimations than the NDVI, representing vegetation.

5.2. Rainfall contribution

To specifically explore the contribution of weather radar rainfall observations on air temperature estimations, this study individually removed rainfall from all local-scale variables while generating the downscaling models by the GP algorithm. Considering the direct correlation between rainfall and soil moisture, the same procedure was applied to soil moisture and its combination with rainfall to explore their effects on model performance, as shown in Table 4. It indicates that rainfall has a significant impact on the performance of the downscaling model, leading to a 0.016 °C reduction in *RMSE* for 2019 and a 0.035 °C reduction for 2022. Furthermore, although removing soil moisture only resulted in a 0.002 °C decrease in *RMSE* for 2019 and 0.017 °C for 2022, the reduction in *RMSE* caused by simultaneously removing both soil moisture and rainfall was 0.025 °C in 2019 and 0.066 °C in 2022, exceeding the sum of their individual impacts.

5.3. Impact of meteorological-station spatial density

Fig. 8 illustrates how changes in weather station density affect the downscaling performance of air temperature. The results from 2019 and 2022 exhibit a similar trend: as the density decreases from 1.6 stations/ 100 km^2 to 0.1 stations/100 km^2, the downscaling performance gradually decreases. Moreover, when the density exceeds the threshold of 0.5 stations/100 km^2 (22 stations in this research), increasing station density becomes less effective in further improving the performance of the downscaling models. On average, each addition of five weather stations

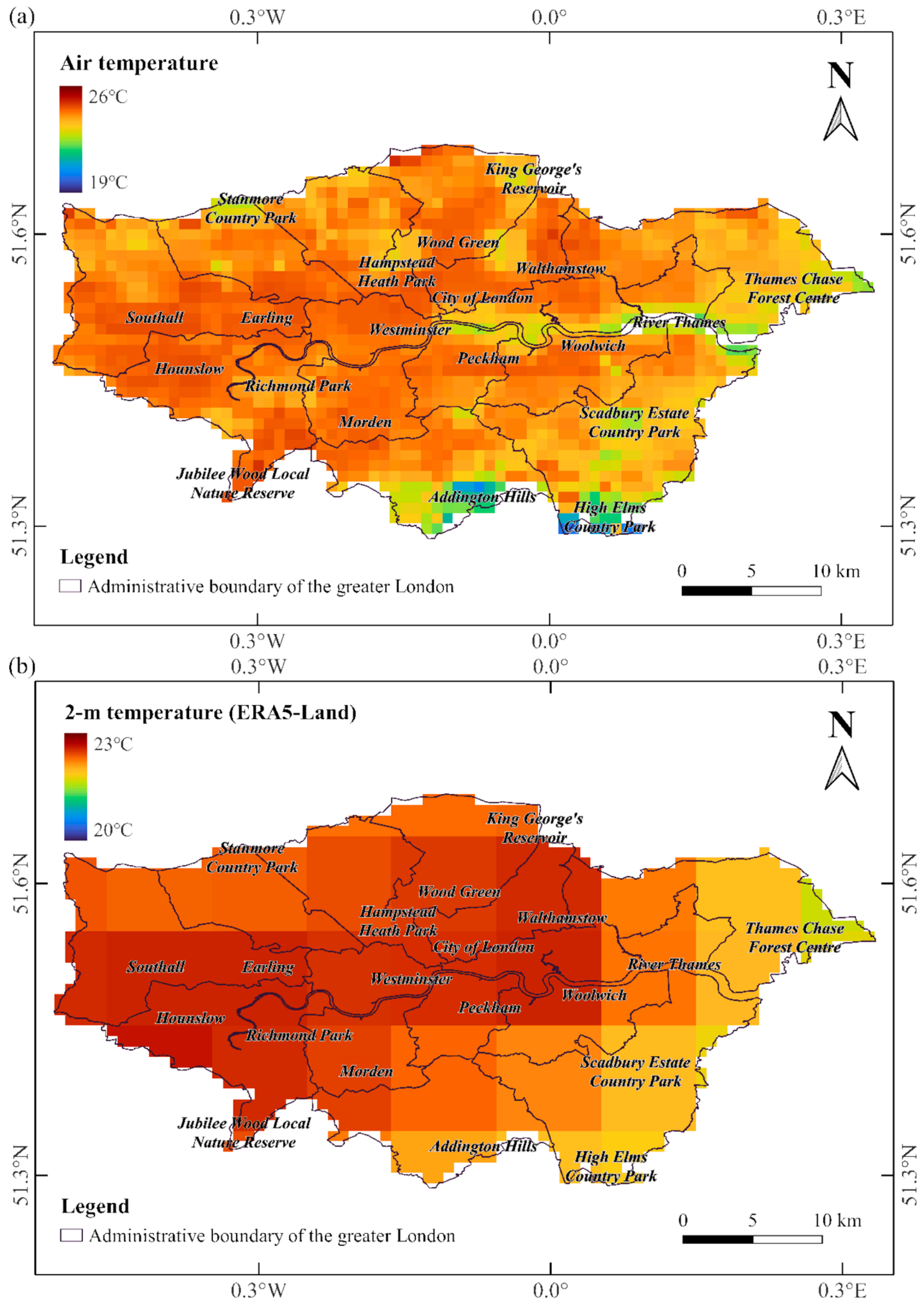

Fig. 7. The spatial distribution pattern across London on 4 July 2019 at 14:00: (a) air temperature from the optimal downscaling model; (b) 2-m temperature from the ERA5-Land; (c) elevation; (d) emissivity; (e) MNDWI; (f) NDVI.

only increases the *R-squared* value by 0.005 and decreases the *RMSE* by 0.027°C.

6. Discussions

The limited availability of high spatiotemporal resolution air temperature data hinders the monitoring of spatial variations in temperature during heatwaves within urban areas (Yoo et al., 2023). Based on crowdsourced weather station observations, our statistical downscaling framework utilized the GP algorithm to integrate satellite products, reanalysis datasets, and weather radar observations to obtain 1-km daytime hourly air temperatures. For 2019, the model achieved an *R-squared* value of 0.867, an *RMSE* of 1.694 °C, and an *MAE* of 1.276 °C, while for 2022, it attained an *R-squared* value of 0.862, an *RMSE* of 1.785 °C, and an *MAE* of 1.278 °C. Compared to the current focus of scholars on exploring high-resolution daily maximum air temperatures (Dos Santos, 2020; Noi et al., 2016; Yoo et al., 2018), our generated hourly air temperatures can better monitor the spatial distribution changes of high-temperature areas throughout daylight hours, thereby providing a stronger theoretical support for public health authorities to analyse heat-related mortalities and implementing heatwave countermeasures. So far, there has been no study that integrates data from the aforementioned three sources with crowdsourced data from private weather stations to obtain high spatiotemporal resolution air temperatures. It seems to be primarily due to the fact that processing crowdsourced data from private weather stations requires complex QC steps, and the weather radar data of many countries is closed-source.

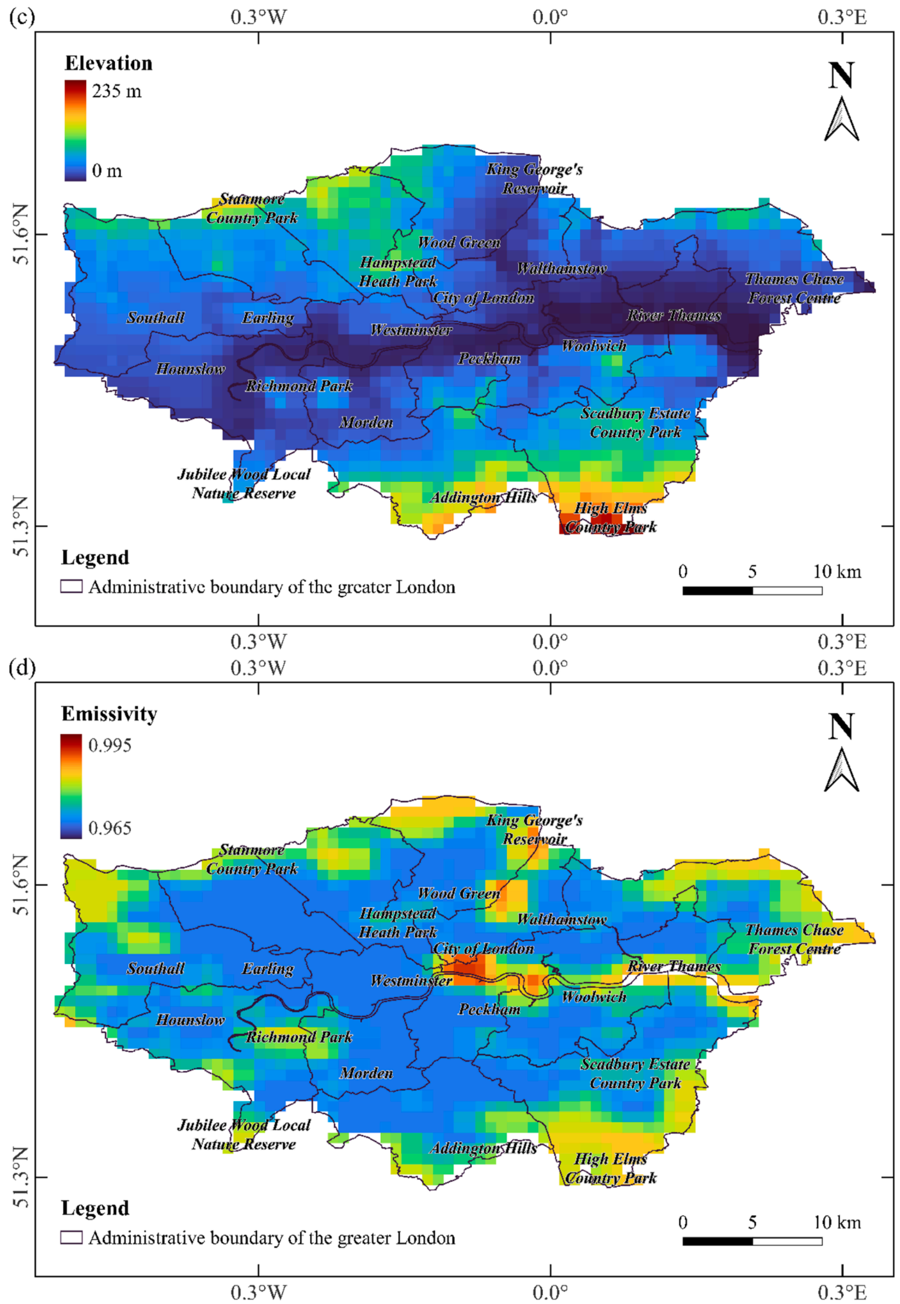

Fig. 7. (*continued*).

6.1. Variable significance

The research of W. Liu et al. (2022) has already demonstrated that rainfall can significantly impact urban air temperatures. Our exploratory analysis further corroborates this finding, with rainfall ranking second only to elevation in terms of its importance for estimating air temperature, as shown in Table 2 and Table 3. Besides, the results in Table 4 demonstrate that compared to using either variable alone, incorporating the coupling of soil moisture and rainfall in the downscaling model can provide a more comprehensive explanation of air temperature variations. This further proves the potential of integrating weather radar observations with other data sources, such as satellite products. However, most existing studies only focused on exploring different fusion methods or algorithms for integrating satellite products and reanalysis datasets to obtain high-resolution temperature data, while neglecting the potential of integrating other data sources (e.g., weather radar). This could be a promising direction for researchers in geoinformatics to obtain high spatiotemporal resolution air temperatures.

Our results also indicate that soil moisture did not exhibit the expected significance in the downscaling regression model, as shown in Table 2. It is mainly due to the high correlation between soil moisture and 2-m temperature from ERA5-Land, as shown in Fig. 5. The close relationship between soil moisture and 2-m temperature can cause relatively high collinearity, leading to a lower contribution of soil moisture in the regression model. However, considering the contribution of the coupled effects with other variables (e.g., rainfall) to the downscaling model, incorporating soil moisture for estimating air temperatures is still considered meaningful.

Additionally, while water bodies and green spaces have similar emissivity values obtained from MODIS, water bodies actually have a superior cooling effect compared to green spaces (Tan et al., 2021; Yu et al., 2020), especially flowing water bodies (Deng et al., 2023). It may

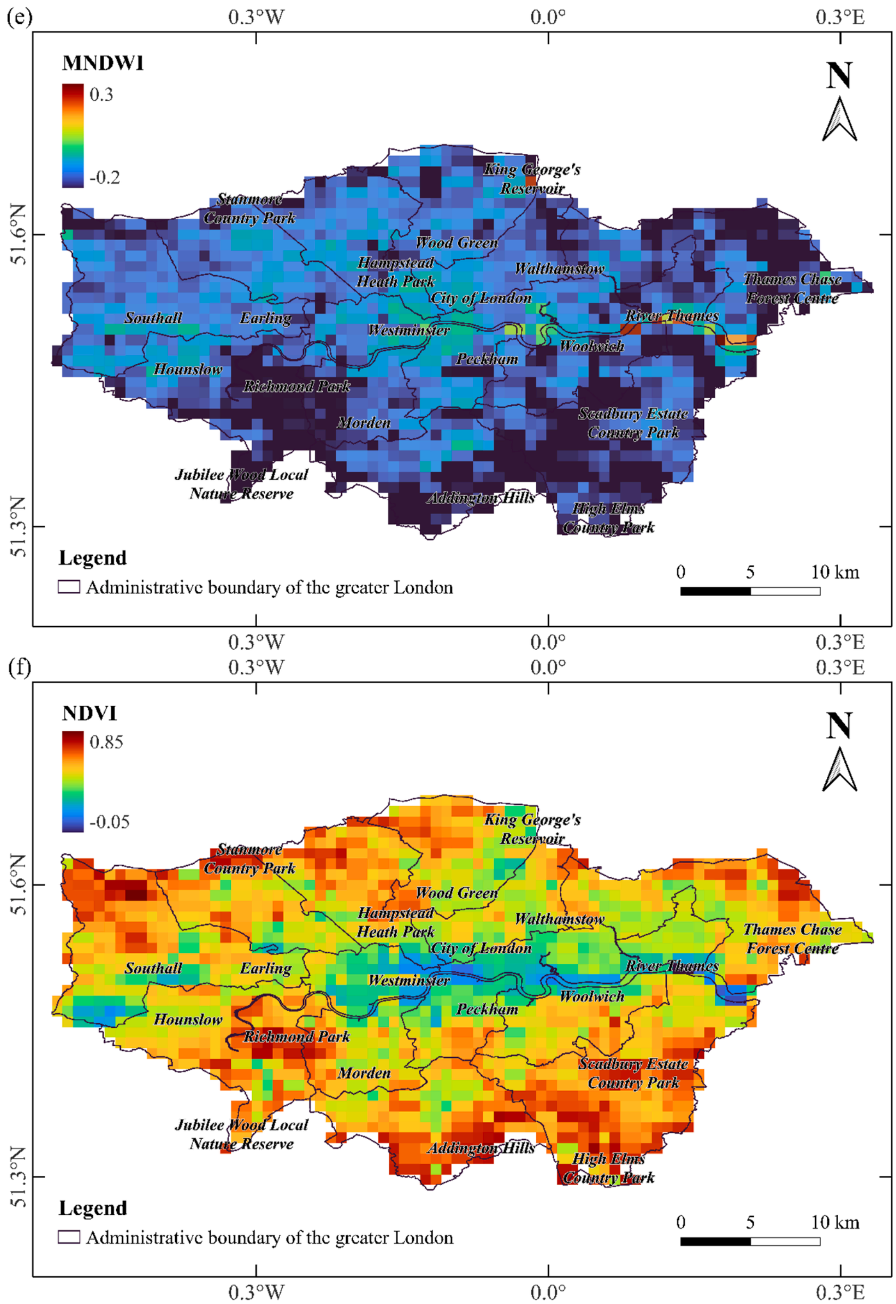

Fig. 7. (*continued*).

Table 4
Performance of the air temperature downscaling modele while removing rainfall and soil moisture.

Year		Remove rainfall and soil moisture	Remove rainfall	Remove soil moisture	All variables
2019	*R-squared*	0.863	0.864	0.866	0.867
	RMSE	1.719	1.710	1.696	1.694
	MAE	1.296	1.290	1.278	1.276
2022	*R-squared*	0.855	0.857	0.860	0.862
	RMSE	1.851	1.820	1.802	1.785
	MAE	1.337	1.312	1.297	1.278

explain why MNDWI exhibits greater significance than NDVI, whether in downscaling models (Table 2) or Pearson correlation results (Fig. 5). Fig. 7a also illustrates a similar scenario, showing that compared to parks within London, the River Thames has a more significant cooling effect on its surroundings.

6.2. Spatial distribution of air temperature

The spatial distribution pattern of air temperature across London in Fig. 7a indicates that different land attributes can have varying cooling or warming effects on air temperatures at the local level. In this research, built-up areas have been found to have a warming effect on air temperature. Compared to rural areas, these areas typically have less green space and more impermeable surfaces (Oke, 1982). This leads to a reduction in evapotranspiration and latent heat flux in urban areas, converting more energy into sensible heat and finally resulting in

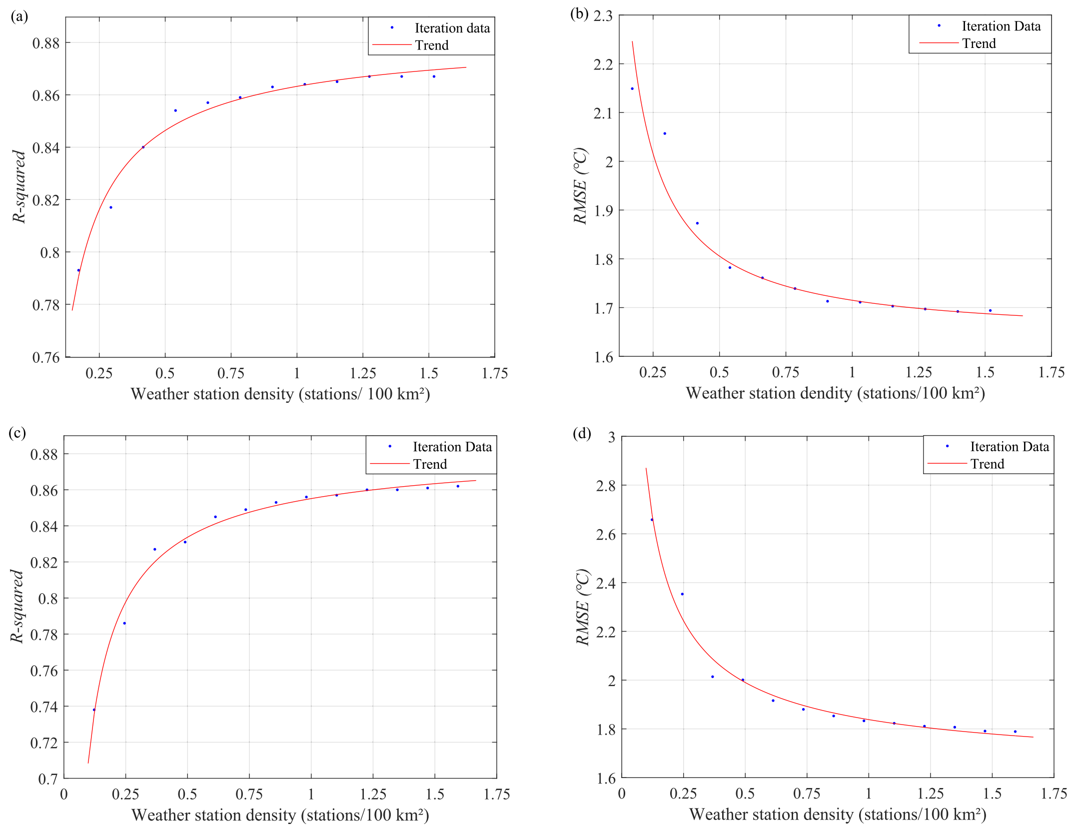

Fig. 8. Performance statistics for air temperature downscaling after iteratively removing randomly selected weather stations: (a) R-squared results for summer 2019; (b) RMSE results for summer 2019; (c) R-squared results for summer 2022; (d) RMSE results for summer 2022.

warming air temperatures (Grimmond & Oke, 1991). Additionally, heat released from human activities such as traffic further exacerbates this warming effect (Allen et al., 2011). The high temperatures observed in densely populated residential areas (e.g., Earling, Woolwich, Hounslow, and Peckham) provide strong evidence for this effect. For the cooling effect, areas with high vegetation coverage, high elevation, or abundant water bodies have been found to be significant contributors to air temperature reduction at the local level. Especially for the areas with high vegetation coverage and abundant water bodies, as important components of blue-green infrastructure (Z. Liu et al., 2021), they have been widely acknowledged as effective in reducing the negative impacts of heatwaves. Areas with high vegetation coverage achieve cooling by shading, guiding airflows, and intercepting precipitation (Gatto et al., 2020; Morakinyo et al., 2017), while water bodies cool the overlying and adjacent air through evaporation and convection (Albdour & Baranyai, 2019; Jacobs et al., 2020). The distribution of low air temperatures observed in blue-green infrastructure areas such as the River Thames, Addington Hill, Thames Chase Forest Centre, and High Elms Country Park in Fig. 7 also confirms this phenomenon. These findings provide actionable insights for urban planners, who can use such high-resolution patterns to prioritise the design and placement of blue-green infrastructure in neighbourhoods with high air temperatures to improve urban heatwave resilience.

However, our results note that the above patterns are not always effective in downscaling. For instance, Jubilee Wood Local Nature Reserve and Southall, as shown in Fig. 7, exhibit anomalously high temperatures. Comparing the spatial distribution of generated air temperatures (Fig. 7a) and 2-m temperatures from ERA5-Land (Fig. 7b), it can be observed that areas with anomalously high temperatures are mainly influenced by the spatial distribution characteristics of 2-m temperature, which is regarded as the larger-scale variable in the downscaling model. Although the ERA5-Land dataset has been shown to have high accuracy at the regiona-scale in previous studies (Huang et al., 2021; Yilmaz, 2023), the complex urban surface can lead to significant spatial differences at the local scale (Zou et al., 2022). Moreover, the land scheme of ERA5-Land does not specifically account for urban areas (Schwingshackl et al., 2023), which may result in the inadequate capture of the spatial variation of air temperatures at the city level. Thus, the spatial distributions of 2-m temperature may not adequately represent the air temperature distributions in urban areas, inevitably resulting in areas with abnormal air temperature during the downscaling process.

Moreover, the downscaling method itself also contributes to the emergence of anomalous temperature patterns. A comparison between Fig. 7(a) and Fig. 7(b) reveals that, while downscaling improves spatial resolution, it inevitably introduces visible horizontal and vertical line patterns near the original 0.1° pixel boundaries. This issue arises because our downscaling approach relies on low-resolution large-scale variables (i.e., ERA5-Land 0.1° air temperature) to generate high-resolution (1-km) air temperatures. However, it does not incorporate constraints to ensure smooth transitions between adjacent pixels, resulting in abrupt temperature changes at pixel boundaries and leading to grid artifacts (Wilby & Wigley, 1997). This is a common limitation of downscaling methods, as also noted in the research of Wen et al. (2023). Thus, for future research, explore the integration of appropriate smoothing models during the data preprocessing stage may effectively mitigate the anomalous temperature patterns observed in the downscaled results.

6.3. The prospects of crowd-sourced air temperature observations

In the downscaling process of this study, we found that the accuracy of the high spatiotemporal resolution air temperatures generated by the downscaling model significantly improves as the density of weather stations increases, particularly when the density is below approximately 0.5 stations per 100 km^2. Currently, the density of private weather stations in many cities in Europe, the Americas, and Oceania meets this threshold (Hahn et al., 2022; Venter et al., 2020). This can effectively address a significant issue encountered in constructing statistical climate models: how to ensure that the number of weather stations used in the research is sufficient for the study area (Bustos et al., 2015; Mahmood et al., 2010). Moreover, the findings can also offer valuable references for researchers in geoinformatics seeking to improve the computational efficiency of downscaling methods by considering the spatial density of observational data.

Furthermore, previous studies have compared their methods for obtaining high-resolution air temperatures with those proposed by other research institutions, have only simply compared the performance of different models (e.g., *RMSE*, *R-squared*) without considering the influence of weather station density (Dos Santos, 2020; Flückiger et al., 2022; Kloog et al., 2014). Our study, along with research conducted by Venter et al. (2020), demonstrated the importance of weather station density in improving model performance. Therefore, judging performance solely through model comparisons lacks a comprehensive assessment. Comparative analysis should be conducted while controlling for variables such as weather station density to enhance credibility.

7. Conclusions

Based on crowd-sourced air temperature observations from private weather stations, the study made the first attempt to generate hourly air temperatures for London during summer daytime by integrating satellite products, reanalysis datasets, and weather radar observations. The model utilised 2-meter temperature data from ERA5-Land as the larger-scale variable and employed the GP algorithm to integrate other local-scale variables for generating the optimal downscaling model to obtain high spatiotemporal resolution air temperatures. The generated model demonstrated good performance in both research periods. For 2019, it achieved an *R-squared* value of 0.867, an *RMSE* of 1.694 °C, and an *MAE* of 1.276 °C, while for 2022, it attained an *R-squared* value of 0.862, an *RMSE* of 1.785 °C, and an *MAE* of 1.278 °C. These results indicate that the combination of satellite products, reanalysis datasets, weather radar observations, and crowd-sourced air temperatures is beneficial. High spatiotemporal resolution rainfall data from weather radar observations significantly impacts the accuracy of generated air temperatures, second only to elevation. However, existing studies often overlook the importance of weather radar observations in estimating air temperatures. Furthermore, the study observed that blue-green infrastructure in urban areas, particularly water bodies, can significantly cool air temperatures in densely populated built-up areas. Therefore, constructing blue-green infrastructure centred around water bodies in the future could be an effective measure to enhance urban heatwave resilience.

Technically, our downscaling framework can be applied to any city with access to weather radar rainfall observations and a sufficient number of weather stations. It is worth noting that for research aiming to obtain 1-km resolution air temperatures, we recommend a minimum of 0.5 stations per 100 km^2 to enhance the accuracy of the model. For studies aiming to compare the advantages and disadvantages of different methods, considering the impact of weather station density on model accuracy, constructing models for comparison based on stations with similar densities is considered more convincing than simply comparing the performance of different models. The study also found that using 2-m temperature from ERA5-Land as the larger-scale variable in the downscaling model may not capture significant spatial differences caused by the complex urban surface. Therefore, the spatial distribution of the generated air temperatures by the model would inevitably be influenced by the inherent errors of the ERA5-Land dataset. Moreover, the grid artifacts introduced by the downscaling method further exacerbate the anomalous temperature patterns. Therefore, addressing these limitations could be a promising direction for future model optimization.

Overall, our study explored the contributions of weather radar observations and weather station density to high spatiotemporal resolution air temperature estimations, providing possible directions for researchers to further improve air temperature estimation models in the future. In addition, the generated high-resolution air temperature data can also help urban planners and public health authorities more accurately identify heat-vulnerable areas, support the adaptive design of blue-green infrastructure, and enhance the effectiveness of urban resilience planning.

CRediT authorship contribution statement

Zitong Wen: Writing – original draft, Visualization, Validation, Software, Methodology, Investigation, Formal analysis, Conceptualization. **Lu Zhuo:** Writing – review & editing, Supervision, Resources, Project administration, Conceptualization. **Meiling Gao:** Writing – review & editing, Supervision. **Dawei Han:** Writing – review & editing, Supervision, Resources, Project administration, Funding acquisition, Conceptualization.

Declaration of competing interest

The authors declare that they have no known competing financial interests or personal relationships that could have appeared to influence the work reported in this paper.

Data availability

Data will be made available on request.

References

Abera, T.A., Heiskanen, J., Pellikka, P.K., Maeda, E.E., 2020. Impact of rainfall extremes on energy exchange and surface temperature anomalies across biomes in the Horn of Africa. Agricultural Forest Meteorology 280, 107779. https://doi.org/10.1016/j.agrformet.2019.107779.

Abonyi, J. (2022). Genetic Programming MATLAB Toolbox. MATLAB Central File Exchange. Retrieved 3 December, 2022, from https://www.mathworks.com/matlabcentral/fileexchange/47197-genetic-programming-matlab-toolbox.

Albdour, M.S., Baranyai, B., 2019. Water body effect on microclimate in summertime: A case study from Pécs. Pollack Periodica 14 (3), 131–140. https://doi.org/10.1556/606.2019.14.3.13.

Allen, L., Lindberg, F., Grimmond, C., 2011. Global to city scale urban anthropogenic heat flux: model and variability. Int. J. Climatol. 31 (13), 1990–2005. https://doi.org/10.1002/joc.2210.

Almeida, M., Coelho, P., 2023. A first assessment of ERA5 and ERA5-Land reanalysis air temperature in Portugal. Int. J. Climatol. 43 (14), 6643–6663. https://doi.org/10.1002/joc.8225.

Anderson, G.B., Bell, M.L., 2011. Heat waves in the United States: mortality risk during heat waves and effect modification by heat wave characteristics in 43 US communities. Environ. Health Perspect. 119 (2), 210–218. https://doi.org/10.1289/ehp.1002313.

Arbuthnott, K.G., Hajat, S., 2017. The health effects of hotter summers and heat waves in the population of the United Kingdom: a review of the evidence. Environ. Health 16, 1–13. https://doi.org/10.1186/s12940-017-0322-5.

Bassett, R., Cai, X., Chapman, L., Heaviside, C., Thornes, J.E., Muller, C.L., Young, D.T., Warren, E.L., 2016. Observations of urban heat island advection from a high-density monitoring network. Q. J. R. Meteorolog. Soc. 142 (699), 2434–2441. https://doi.org/10.1002/qj.2836.

Brousse, O., Simpson, C.H., Kenway, O., Martilli, A., Krayenhoff, S., Zonato, A., Heaviside, C., 2022. Bias correction of modelled urban temperatures with crowd-sourced weather data. Authorea Preprints. https://doi.org/10.1002/essoar.10512277.2.

Bustos, E., Meza, F.J.J.T., Climatology, A., 2015. A method to estimate maximum and minimum air temperature using MODIS surface temperature and vegetation data: application to the Maipo Basin, Chile. Theor. Appl. Climatol. 120, 211–226. https://doi.org/10.1007/s00704-014-1167-2.

Carrión, D., Arfer, K.B., Rush, J., Dorman, M., Rowland, S.T., Kioumourtzoglou, M.-A., Kloog, I., Just, A.C., 2021. A 1-km hourly air-temperature model for 13 northeastern US states using remotely sensed and ground-based measurements. Environ. Res. 200, 111477. https://doi.org/10.1016/j.envres.2021.111477.

Cerlini, P.B., Silvestri, L., Saraceni, M., 2020. Quality control and gap-filling methods applied to hourly temperature observations over central Italy. Meteorol. Appl. 27 (3), e1913. https://doi.org/10.1002/met.1913.

Chapman, L., Bell, C., Bell, S., 2017. Can the crowdsourcing data paradigm take atmospheric science to a new level? A case study of the urban heat island of London quantified using Netatmo weather stations. Int. J. Climatol. 37 (9), 3597–3605. https://doi.org/10.1002/joc.4940.

Clarke, B., Otto, F., Stuart-Smith, R., Harrington, L., 2022. Extreme weather impacts of climate change: an attribution perspective. Environ. Res.: Clim. 1 (1), 012001. https://doi.org/10.1088/2752-5295/ac6e7d.

Coll, C., Wan, Z., Galve, J.M., 2009. Temperature-based and radiance-based validations of the V5 MODIS land surface temperature product. J. Geophys. Res. Atmos. 114 (D20). https://doi.org/10.1029/2009JD012038.

Deng, Z., Zhao, H., Li, L., Liu, G., Lin, H., Devlin, A.T., 2023. The climate adaptive characteristics of urban inside/outside water bodies based on their cooling effect in Poyang and Dongting lake regions. China. Heliyon 9 (5). https://doi.org/10.1016/j.heliyon.2023.e15974.

Didari, S., Zand-Parsa, S., 2018. Enhancing estimation accuracy of daily maximum, minimum, and mean air temperature using spatio-temporal ground-based and remote-sensing data in southern Iran. Int. J. Remote Sens. 39 (19), 6316–6339. https://doi.org/10.1080/01431161.2018.1460500.

Dos Santos, R.S., 2020. Estimating spatio-temporal air temperature in London (UK) using machine learning and earth observation satellite data. International Journal of Applied Earth Observation Geoinformation 88, 102066. https://doi.org/10.1016/j.jag.2020.102066.

Ferreira, M.J., de Oliveira, A.P., Soares, J., Codato, G., Bárbaro, E.W., Escobedo, J.F., 2012. Radiation balance at the surface in the city of São Paulo, Brazil: diurnal and seasonal variations. Theor. Appl. Climatol. 107, 229–246. https://doi.org/10.1007/s00704-011-0480-2.

Flückiger, B., Kloog, I., Ragettli, M.S., Eeftens, M., Röösli, M., de Hoogh, K., 2022. Modelling daily air temperature at a fine spatial resolution dealing with challenging meteorological phenomena and topography in Switzerland. Int. J. Climatol. 42 (12), 6413–6428. https://doi.org/10.1002/joc.7597.

Fouillet, A., Rey, G., Wagner, V., Laaidi, K., Empereur-Bissonnet, P., Le Tertre, A., Frayssinet, P., Bessemoulin, P., Laurent, F., De Crouy-Chanel, P., 2008. Has the impact of heat waves on mortality changed in France since the European heat wave of summer 2003? A study of the 2006 heat wave. Int. J. Epidemiol. 37 (2), 309–317. https://doi.org/10.1093/ije/dym253.

Gandomi, A.H., Roke, D.A., 2015. Assessment of artificial neural network and genetic programming as predictive tools. Adv. Eng. Softw. 88, 63–72. https://doi.org/10.1016/j.advengsoft.2015.05.007.

Gatto, E., Buccolieri, R., Aarrevaara, E., Ippolito, F., Emmanuel, R., Perronace, L., Santiago, J.L., 2020. Impact of urban vegetation on outdoor thermal comfort: Comparison between a mediterranean city (Lecce, Italy) and a northern European city (Lahti, Finland). Forests 11 (2), 228. https://doi.org/10.3390/f11020228.

Gomes, F.M., Pereira, F.M., Silva, A.F., Silva, M.B., 2019. Multiple response optimization: Analysis of genetic programming for symbolic regression and assessment of desirability functions. Knowledge-Based Systems 179, 21–33. https://doi.org/10.1016/j.knosys.2019.05.002.

Gorelick, N., Hancher, M., Dixon, M., Ilyushchenko, S., Thau, D., Moore, R., 2017. Google Earth Engine: Planetary-scale geospatial analysis for everyone. Remote Sens. Environ. 202, 18–27. https://doi.org/10.1016/j.rse.2017.06.031.

Green, H.K., Andrews, N., Armstrong, B., Bickler, G., Pebody, R., 2016. Mortality during the 2013 heatwave in England–how did it compare to previous heatwaves? A retrospective observational study. Environ. Res. 147, 343–349. https://doi.org/10.1016/j.envres.2016.02.028.

Grimmond, C.S.B., Oke, T.R., 1991. An evapotranspiration-interception model for urban areas. Water Resour. Res. 27 (7), 1739–1755. https://doi.org/10.1029/91WR00557.

Gutiérrez-Avila, I., Arfer, K.B., Wong, S., Rush, J., Kloog, I., Just, A.C., 2021. A spatiotemporal reconstruction of daily ambient temperature using satellite data in the Megalopolis of Central Mexico from 2003 to 2019. Int. J. Climatol. 41 (8), 4095–4111. https://doi.org/10.1002/joc.7060.

Hahn, C., Garcia-Marti, I., Sugier, J., Emsley, F., Beaulant, A.-L., Oram, L., Strandberg, E., Lindgren, E., Sunter, M., Ziska, F., 2022. Observations from personal weather stations—EUMETNET interests and experience. Climate 10 (12), 192. https://doi.org/10.3390/cli10120192.

Hajat, S., Kovats, R.S., Atkinson, R.W., Haines, A., 2002. Impact of hot temperatures on death in London: a time series approach. Journal of Epidemiology Community Health 56 (5), 367–372. https://doi.org/10.1136/jech.56.5.367.

Hassani, A., Santos, G.S., Schneider, P., Castell, N., 2023. Interpolation, satellite-based machine learning, or meteorological simulation? A comparison analysis for spatio-temporal mapping of mesoscale urban air temperature. Environ. Model. Assess. 1–16. https://doi.org/10.1007/s10666-023-09943-9.

Hong, C., Qu, Z., Xu, W., Gu, Z., 2023. Study on water cooling island effects under different climatic conditions. City Built Environ. 1 (1), 4. https://doi.org/10.1007/s44213-022-00004-7.

Huang, X., Han, S., Shi, C., 2021. Multiscale Assessments of Three Reanalysis Temperature Data Systems over China. Agriculture 11 (12), 1292. https://doi.org/10.3390/agriculture11121292.

Jacobs, C., Klok, L., Bruse, M., Cortesão, J., Lenzholzer, S., Kluck, J., 2020. Are urban water bodies really cooling? Urban Clim. 32, 100607. https://doi.org/10.1016/j.uclim.2020.100607.

Kaplan, G., Avdan, Z.Y., Avdan, U., 2019. Mapping and monitoring wetland dynamics using thermal, optical, and SAR remote sensing data. Sustainable. Solutions 87. https://doi.org/10.5772/intechopen.80264.

Kloog, I., Nordio, F., Coull, B.A., Schwartz, J., 2014. Predicting spatiotemporal mean air temperature using MODIS satellite surface temperature measurements across the Northeastern USA. Remote Sens. (Basel)of Environment 150, 132–139. https://doi.org/10.1016/j.rse.2014.04.024.

Koc, C.B., Osmond, P., Peters, A., 2018. Evaluating the cooling effects of green infrastructure: A systematic review of methods, indicators and data sources. Sol. Energy 166, 486–508. https://doi.org/10.1016/j.solener.2018.03.008.

Kodama, K. M., Kourkchi, E., Longman, R. J., Lucas, M. P., Bateni, S. M., Huang, Y. F., Kagawa-Viviani, A., Mclean, J., Cleveland, S. B., & Giambelluca, T. W. (2024). Mapping daily air temperature over the Hawaiian Islands from 1990 to 2021 via an optimized piecewise linear regression technique. Earth and Space Science, 11(1), e2023EA002851. https://doi.org/10.1029/2023EA002851.

Lin, S., Moore, N.J., Messina, J.P., DeVisser, M.H., Wu, J., 2012. Evaluation of estimating daily maximum and minimum air temperature with MODIS data in east Africa. International Journal of Applied Earth Observation Geoinformation 18, 128–140. https://doi.org/10.1016/j.jag.2012.01.004.

Liu, W., Dong, S., Zheng, J., Liu, C., Wang, C., Shangguan, W., Zhang, Y., Zhang, Y., 2022. Quantifying the Rainfall Cooling Effect: The Importance of Relative Humidity in Guangdong, South China. Journal of Hydrometeorology 23 (6), 875–889. https://doi.org/10.1175/JHM-D-21-0155.1.

Liu, Z., Cheng, W., Jim, C.Y., Morakinyo, T.E., Shi, Y., Ng, E., 2021. Heat mitigation benefits of urban green and blue infrastructures: A systematic review of modeling techniques, validation and scenario simulation in ENVI-met V4. Build. Environ. 200, 107939. https://doi.org/10.1016/j.buildenv.2021.107939.

Macintyre, H., Heaviside, C., Taylor, J., Picetti, R., Symonds, P., Cai, X.-M., Vardoulakis, S., 2018. Assessing urban population vulnerability and environmental risks across an urban area during heatwaves–Implications for health protection. Sci. Total Environ. 610, 678–690. https://doi.org/10.1016/j.scitotenv.2017.08.062.

Mahmood, R., Pielke Sr, R.A., Hubbard, K.G., Niyogi, D., Bonan, G., Lawrence, P., McNider, R., McAlpine, C., Etter, A., Gameda, S., 2010. Impacts of land use/land cover change on climate and future research priorities. Bull. Am. Meteorol. Soc. 91 (1), 37–46. https://doi.org/10.1175/2009BAMS2769.1.

Meier, F., Fenner, D., Grassmann, T., Otto, M., Scherer, D., 2017. Crowdsourcing air temperature from citizen weather stations for urban climate research. Urban Clim. 19, 170–191. https://doi.org/10.1016/j.uclim.2017.01.006.

Mitchell, T.D., Fry, M.J., 2024. The importance of crowdsourced observations for urban climate services. Int. J. Climatol. 44 (5), 1409–1422. https://doi.org/10.1002/joc.8390.

Mora, C., Dousset, B., Caldwell, I.R., Powell, F.E., Geronimo, R.C., Bielecki, C.R., Counsell, C.W., Dietrich, B.S., Johnston, E.T., Louis, L.V., 2017. Global risk of deadly heat. Nat. Clim. Chang. 7 (7), 501–506. https://doi.org/10.1038/nclimate3322.

Morakinyo, T.E., Dahanayake, K.K.C., Ng, E., Chow, C.L., 2017. Temperature and cooling demand reduction by green-roof types in different climates and urban densities: A co-simulation parametric study. Energ. Buildings 145, 226–237. https://doi.org/10.1016/j.enbuild.2017.03.066.

Murage, P., Kovats, S., Sarran, C., Taylor, J., McInnes, R., Hajat, S., 2020. What individual and neighbourhood-level factors increase the risk of heat-related mortality? A case-crossover study of over 185,000 deaths in London using high-resolution climate datasets. Environ. Int. 134, 105292. https://doi.org/10.1016/j.envint.2019.105292.

Napoly, A., Grassmann, T., Meier, F., Fenner, D., 2018. Development and application of a statistically-based quality control for crowdsourced air temperature data. Front. Earth Sci. 6, 118. https://doi.org/10.3389/feart.2018.00118.

Njoku, E.A., Akpan, P.E., Effiong, A.E., Babatunde, I.O., 2023. The effects of station density in geostatistical prediction of air temperatures in Sweden: A comparison of two interpolation techniques. Resour. Environ. Sustainability 11, 100092. https://doi.org/10.1016/j.resenv.2022.100092.

Noi, P.T., Kappas, M., Degener, J., 2016. Estimating daily maximum and minimum land air surface temperature using MODIS land surface temperature data and ground truth data in Northern Vietnam. Remote Sens. (Basel) 8 (12), 1002. https://doi.org/10.3390/rs8121002.

Oke, T.R., 1982. The energetic basis of the urban heat island. Q. J. R. Meteorolog. Soc. 108 (455), 1–24. https://doi.org/10.1002/qj.49710845502.

Oswald, S.M., Schneider, S., Hahn, C., Žuvela-Aloise, M., Schmederer, P., Wastl, C., Hollosi, B.J.A., 2024. High-Resolution Air Temperature Forecasts in Urban Areas: A Meteorological Perspective on Their Added Value. 15 (12), 1544.

Rooney, G.G., Van Lipzig, N., Thiery, W., 2018. Estimating the effect of rainfall on the surface temperature of a tropical lake. Hydrol. Earth Syst. Sci. 22 (12), 6357–6369. https://doi.org/10.5194/hess-22-6357-2018.

Roshan, G., Moghbel, M., 2020. Quantifying the cooling effect of rain events on outdoor thermal comfort in the southern coastal stations of the Caspian Sea. J. Therm. Biol 93, 102733. https://doi.org/10.1016/j.jtherbio.2020.102733.

Rustemeyer, N., Howells, M., 2021. Excess mortality in England during the 2019 summer heatwaves. Climate 9 (1), 14. https://doi.org/10.3390/cli9010014.

Saaroni, H., Ziv, B., 2010. Estimating the urban heat island contribution to urban and rural air temperature differences over complex terrain: application to an arid city. J. Appl. Meteorol. Climatol. 49 (10), 2159–2166. https://doi.org/10.1175/2010JAMC2473.1.

Sanderson, M.G., Economou, T., Salmon, K.H., Jones, S.E., 2017. Historical trends and variability in heat waves in the United Kingdom. Atmos. 8 (10), 191. https://doi.org/10.3390/atmos8100191.

Schwingshackl, C., Daloz, A.S., Iles, C., Aunan, K., Sillmann, J., 2023. High-resolution projections of ambient heat for major European cities using different heat metrics. Nat. Hazards Earth Syst. Sci. Discuss. 2023, 1–37. https://doi.org/10.5194/nhess-24-331-2024.

Shen, H., Huang, L., Zhang, L., Wu, P., Zeng, C., 2016. Long-term and fine-scale satellite monitoring of the urban heat island effect by the fusion of multi-temporal and multi-sensor remote sensed data: A 26-year case study of the city of Wuhan in China. Remote Sens. Environ. 172, 109–125. https://doi.org/10.1016/j.rse.2015.11.005.

Shen, H., Jiang, Y., Li, T., Cheng, Q., Zeng, C., Zhang, L., 2020. Deep learning-based air temperature mapping by fusing remote sensing, station, simulation and socioeconomic data. Remote Sens. Environ. 240, 111692. https://doi.org/10.1016/j.rse.2020.111692.

Shi, L., Liu, P., Kloog, I., Lee, M., Kosheleva, A., Schwartz, J., 2016. Estimating daily air temperature across the Southeastern United States using high-resolution satellite data: A statistical modeling study. Environ. Res. 146, 51–58. https://doi.org/10.1016/j.envres.2015.12.006.

Shiflett, S.A., Liang, L.L., Crum, S.M., Feyisa, G.L., Wang, J., Jenerette, G.D., 2017. Variation in the urban vegetation, surface temperature, air temperature nexus. Sci. Total Environ. 579, 495–505. https://doi.org/10.1016/j.scitotenv.2016.11.069.

Sokol, Z., Szturc, J., Orellana-Alvear, J., Popova, J., Jurczyk, A., Célleri, R., 2021. The role of weather radar in rainfall estimation and its application in meteorological and hydrological modelling—A review. Remote Sens. (Basel) 13 (3), 351. https://doi.org/10.3390/rs13030351.

Stathopoulou, M., Cartalis, C., Petrakis, M., 2007. Integrating Corine Land Cover data and Landsat TM for surface emissivity definition: application to the urban area of Athens. Greece. International Journal of Remote Sensing 28 (15), 3291–3304. https://doi.org/10.1080/01431160600993421.

Tan, X., Sun, X., Huang, C., Yuan, Y., Hou, D., 2021. Comparison of cooling effect between green space and water body. Sustain. Cities Soc. 67, 102711. https://doi.org/10.1016/j.scs.2021.102711.

Thompson, R., Landeg, O., Kar-Purkayastha, I., Hajat, S., Kovats, S., O'connell, E., 2022. Heatwave mortality in summer 2020 in England: An observational study. International Journal of Environmental Research Public Health 19 (10), 6123. https://doi.org/10.3390/ijerph19106123.

Tsin, P.K., Knudby, A., Krayenhoff, E.S., Ho, H.C., Brauer, M., Henderson, S.B., 2016. Microscale mobile monitoring of urban air temperature. Urban Clim. 18, 58–72. https://doi.org/10.1016/j.uclim.2016.10.001.

Vancutsem, C., Ceccato, P., Dinku, T., Connor, S.J., 2010. Evaluation of MODIS land surface temperature data to estimate air temperature in different ecosystems over Africa. Remote Sens. Environ. 114 (2), 449–465. https://doi.org/10.1016/j.rse.2009.10.002.

Vautard, R., van Aalst, M., Boucher, O., Drouin, A., Haustein, K., Kreienkamp, F., Van Oldenborgh, G.J., Otto, F.E., Ribes, A., Robin, Y., 2020. Human contribution to the record-breaking June and July 2019 heatwaves in Western Europe. Environ. Res. Lett. 15 (9), 094077. https://doi.org/10.1088/1748-9326/aba3d4.

Venter, Z.S., Brousse, O., Esau, I., Meier, F., 2020. Hyperlocal mapping of urban air temperature using remote sensing and crowdsourced weather data. Remote Sens. Environ. 242, 111791. https://doi.org/10.1016/j.rse.2020.111791.

Wang, J., Xu, C., Hu, M., Li, Q., Yan, Z., Zhao, P., Jones, P., 2014. A new estimate of the China temperature anomaly series and uncertainty assessment in 1900–2006. J. Geophys. Res. Atmos. 119 (1), 1–9. https://doi.org/10.1002/2013JD020542.

Wang, M., Wei, J., Wang, X., Luan, Q., Xu, X., 2024. Reconstruction of all-sky daily air temperature datasets with high accuracy in China from 2003 to 2022. Sci. Data 11 (1), 1133. https://doi.org/10.1038/s41597-024-03980-z.

Wen, Z., Zhuo, L., Wang, Q., Wang, J., Liu, Y., Du, S., Abdelhalim, A., Han, D., 2023. Data Fusion for Estimating High-Resolution Urban Heatwave Air Temperature. 15 (16), 3921. https://doi.org/10.3390/rs15163921.

Wilby, R.L., Wigley, T.M., 1997. Downscaling general circulation model output: a review of methods and limitations. Prog. Phys. Geogr. 21 (4), 530–548. https://doi.org/10.1177/030913339702100403.

WMO. (1993). Guide on the Global Data-processing System. (9263133050). World Meteorological Organization.

Xu, H., 2006. Modification of normalised difference water index (NDWI) to enhance open water features in remotely sensed imagery. Int. J. Remote Sens. 27 (14), 3025–3033. https://doi.org/10.1080/01431160600589179.

Xu, Z., FitzGerald, G., Guo, Y., Jalaludin, B., Tong, S., 2016. Impact of heatwave on mortality under different heatwave definitions: a systematic review and meta-analysis. Environ. Int. 89, 193–203. https://doi.org/10.1016/j.envint.2016.02.007.

Yan, H., Zhang, J., Hou, Y., He, Y., 2009. Estimation of air temperature from MODIS data in east China. Int. J. Remote Sens. 30 (23), 6261–6275. https://doi.org/10.1080/01431160902842375.

Yilmaz, M., 2023. Accuracy assessment of temperature trends from ERA5 and ERA5-Land. Sci. Total Environ. 856, 159182. https://doi.org/10.1016/j.scitotenv.2022.159182.

Yin, Q., Wang, J., 2017. The association between consecutive days' heat wave and cardiovascular disease mortality in Beijing. China. BMC Public Health 17 (1), 1–9.

Yoo, C., Im, J., Park, S., Quackenbush, L.J., 2018. Estimation of daily maximum and minimum air temperatures in urban landscapes using MODIS time series satellite data. ISPRS Journal of Photogrammetry Remote Sensing 137, 149–162.

Yoo, C., Im, J., Weng, Q., Cho, D., Kang, E., Shin, Y., 2023. Diurnal urban heat risk assessment using extreme air temperatures and real-time population data in Seoul. Iscience 26 (11), 108123. https://doi.org/10.1016/j.isci.2023.108123.

Yu, Z., Yang, G., Zuo, S., Jørgensen, G., Koga, M., Vejre, H., 2020. Critical review on the cooling effect of urban blue-green space: A threshold-size perspective. Urban For. Urban Green. 49, 126630. https://doi.org/10.1016/j.ufug.2020.126630.

Yule, E.L., Hegerl, G., Schurer, A., Hawkins, E., 2023. Using early extremes to place the 2022 UK heat waves into historical context. Atmos. Sci. Lett. 24 (7), e1159. https://doi.org/10.1002/asl.1159.

Zhang, X., Huang, T., Gulakhmadov, A., Song, Y., Gu, X., Zeng, J., Huang, S., Nam, W.-H., Chen, N., Niyogi, D., 2022. Deep Learning-Based 500 m Spatio-Temporally Continuous Air Temperature Generation by Fusing Multi-Source Data. Remote Sens. (Basel) 14 (15), 3536. https://doi.org/10.3390/rs14153536.

Zhang, Y., Li, J., Liu, D., 2024. Spatial Downscaling of ERA5 Reanalysis Air Temperature Data Based on Stacking Ensemble Learning. Sustainability 16 (5), 1934. https://doi.org/10.3390/su16051934.

Zhang, Z., Du, Q., 2022. Hourly mapping of surface air temperature by blending geostationary datasets from the two-satellite system of GOES-R series. ISPRS Journal of Photogrammetry Remote Sensing 183, 111–128. https://doi.org/10.1016/j.isprsjprs.2021.10.022.

Zhao, P., He, Z., Ma, D., Wang, W., 2023. Evaluation of ERA5-Land reanalysis datasets for extreme temperatures in the Qilian Mountains of China. Frontiers in Ecology Evolution 11, 1135895. https://doi.org/10.3389/fevo.2023.1135895.

Zhou, B., Erell, E., Hough, I., Shtein, A., Just, A.C., Novack, V., Rosenblatt, J., Kloog, I., 2020. Estimation of hourly near surface air temperature across Israel using an ensemble model. Remote Sens. (Basel) 12 (11), 1741. https://doi.org/10.3390/rs12111741.

Zhu, W., Lű, A., Jia, S., 2013. Estimation of daily maximum and minimum air temperature using MODIS land surface temperature products. Remote Sens. Environ. 130, 62–73. https://doi.org/10.1016/j.rse.2012.10.034.

Zou, J., Lu, N., Jiang, H., Qin, J., Yao, L., Xin, Y., Su, F., 2022. Performance of air temperature from ERA5-Land reanalysis in coastal urban agglomeration of Southeast China. Sci. Total Environ. 828, 154459. https://doi.org/10.1016/j.scitotenv.2022.154459.